

1 **Comparative Analysis of MODIS, MISR and AERONET Climatology**
2 **over the Middle East and North Africa**

3 **Ashraf Farahat**

4 Department of Physics, King Fahd University of Petroleum and Minerals, Dhahran 31261,
5 Saudi Arabia;
6 E-Mails: farahata@kfupm.edu.sa

7 *Author to whom correspondence should be addressed; E-Mail: farahata@kfupm.edu.sa.

8 Tel: (321) 541-7088

9
10 **Abstract:**

11 Comparative analysis of MISR, MODIS, and AERONET AOD products performed over
12 seven AERONET stations located in the Middle East and North Africa for the period of 2000
13 – 2015. Sites are categorized into dust, biomass burning and mixed. MISR and MODIS
14 AODs agree during high dust seasons but MODIS tends to underestimate AODs during low
15 dust seasons. Over dust dominating sites, MODIS/Terra AOD indicates a negative trend over
16 the time series, while MODIS/Aqua, MISR, and AERONET depict a positive trend. A
17 deviation between MODIS/Aqua and MODIS/Terra was observed regardless of the
18 geographic location and data sampling. The performance of MODIS is similar over all region
19 with ~68% of AODs within the $\Delta\tau = \pm 0.05 \pm 0.15\tau_{AERO}$ confidence range. MISR AOD
20 retrievals fall within 72% of the same confidence range for all sites examined here. Both
21 MISR and MODIS capture aerosol climatology; however few cases were observed where
22 one of the two sensors better captures the climatology over a certain location or AOD range
23 than the other sensor.

24 **Keywords:** AOD; Remote Sensing; North Africa; Middle East; Validation

25

26

27

28 1. Introduction

29 The Middle East and North Africa host the largest dust source in the world, the Sahara Desert
30 in North Africa that may be responsible for up to 18 percent of global dust emission (Todd
31 et al., 2007, Bou Karam et al. 2010, Schepanski et al. 2016). The vast 650,000 km² Rub' al
32 Khali (Empty Quarter) sand desert is a major source of frequent dust outbreaks and severe
33 dust storms that has major effects on human activities in the Arabian (Böer, 1997 Elagib and
34 Addin 1997, Farahat et al., 2015).

35 Air quality over the Arabian Peninsula has received significant attention during the past 15
36 years due to unprecedented overall economic growth, and a booming oil and gas industry,
37 however, air pollution studies are still far from complete. Frequently blowing dust storms
38 play a significant role in pollutant transport over the Arabian Peninsula; and major
39 environmental pollution events such as burning of Kuwait oil fields during the 1991, Gulf
40 War resulted in a large environmental impact on the Arabian Gulf Area Sadiq and McCain
41 (1993) and Farahat 2016.

42 Aerosol optical depth, AOD, is a parameter to measure the extinction of a beam of light as it
43 passes through a layer of atmosphere that contains aerosols. Both satellites and ground-based
44 instrument can be used to measure AOD in the atmosphere, but within the same temporal
45 coordinates and geographic location different instrument could generate different retrievals
46 Kahn et al., 2007, Kokhanovsky et al., 2007, Liu et al., 2008 and Mishchenko et al., 2009.

47 Since the turn of the 21st century, an upward trend of remotely sensed and ground-based
48 AOD and air pollutants was observed over the Middle East and North Africa (El-Askary
49 2009, Ansmann et al. 2011, Yu et al. 2013, Chin et al. 2014, Yu et al. 2015, Farahat et al.
50 2016, Solomos et al. 2017). This positive trend is attributed to the increase in the Middle
51 Eastern dust activity (Hsu et al., 2012) due to changes in wind speed and soil moisture Ginoux
52 et al. 2001 and Kim et al. 2013. (Yu et al., 2015) concluded that the persistent of the La Niña

Deleted: y

Deleted: Peninsula

Deleted: (also called aerosol optical thickness, AOT)

Deleted: a

Deleted: parameter indicates the

Deleted: radiation

59 conditions (Hoell et al., 2013) have caused increment in Saudi Arabian dust activity during 2008
60 – 2012. Energy subsidies also encourages over energy consumption in the Middle East and
61 North Africa with little incentive to adopt cleaner technology. Lack of applying strict
62 environmental regulations have permitted exacerbated urban air pollution.

63 During the last two decades, a large number of satellites, ground stations and computational
64 models contributed to build global and regional maps for the temporal and spatial aerosol
65 distributions. While, ground-based stations and field measurements can identify aerosols
66 properties over specific geographic locations, the sparse and non-continues data from ground-
67 based sensors scattered over the Middle East and North Africa is not sufficient to provide
68 information on spatial and temporal trends of particulate pollution. On the other hand,
69 satellites imagery could provide a significant source of data mapping over larger areas.

70 For its wide spatial and temporal data availability space-borne sensors are important sources
71 to understand aerosols characteristics and transport, however low sensitivity to particle type
72 under some physical conditions, high surface reflectivity, persistent cloud, and generally low
73 aerosol optical depth could limit satellite data application in characterizing properties of
74 airborne particles, especially in the Middle East.

75 In order to evaluate the efficiency of space-borne sensors in representing ground observations
76 recorded by AERONET stations we have performed detailed statistical inter-comparison analysis
77 between satellite AOD products and AERONET for seven stations in the Middle East and North
78 Africa representative for dust, biomass burning, and mixed aerosol conditions (Dubovik et al.,
79 (2000, 2002, 2006), Holben et al. (2001), Derimian et al., (2006), Basart et al. (2009), Eck
80 el. (2010), Marey et al., 2010, Abdi et al., (2012)). Previously we analysed these seven
81 AERONET stations to understand particles categorization and absorption properties (Farahat
82 et al. 2016), and the current study extends the analysis to the satellite datasets.

83 In the first part of this article, we validated MISR and MODIS retrievals against collocated
84 AERONET observations. We also assessed the consistency in aerosol trends between space-
85 borne sensors and ground-based data.

86 In the second part, we evaluated representativeness of satellite-derived aerosol climatology
87 over the study region from the long-term AERONET data for MISR and MODIS AOD
88 products. It is especially relevant for the MISR instrument, as its sampling is limited by once
89 per week observations of the same region from the two overlapping paths. MODIS provides
90 nearly daily observations to the same geographic location; however, the quality of the product
91 diminishes over the bright targets potentially affecting MODIS-derived aerosol climatology.
92 The collocated MISR, MODIS and AERONET data were obtained at the MAPSS website
93 (<http://giovanni.gsfc.nasa.gov/mapss.html>).

94

95 **2. Materials and Methods**

96 **2.1 MISR**

97 The Multi-angle Imaging SpectroRadiometer (MISR) instrument to measures tropospheric
98 aerosol characteristics through the acquisition of global multi-angle imagery on the daylight
99 side of Earth. MISR applies nine Charge Coupled Devices (CCDs), each with 4 independent
100 line arrays positioned at nine view angles spread out at nadir, 26.1°, 45.6°, 60.0°, and 70.5°.
101 In each of the nine MISR cameras, images are obtained from reflected and scattered sunlight
102 in 4 bands blue, green, red, and near-infrared with a centre wavelength value of 446, 558,
103 672, and 867 nm respectively. The combination of viewing cameras and spectral wavelengths
104 enables MISR to retrieve aerosols AOD over high reflection surfaces like deserts.

105 In this study, we use MISR version 22 (V22) AOD retrievals at 558 nm (green band)
106 measured by MISR instrument with a 17.6 km resolution aboard the Terra satellite. MISR
107 Level 2 aerosol retrievals use only data that pass angle-to-angle smoothness and spatial
108 correlation tests (Martonchik et al. 2002), as well as stereoscopically derived cloud masks

Deleted: Level 2 (ver. 0022)

110 and adaptive cloud-screening brightness thresholds (Zhao and Di Girolamo, 2004). MISR
111 version 23 (V23) retrievals, released on February 2018, was not used in this study, as it has
112 few known issues with the new product that are still under formal validation. Some of these
113 known issues are related to data reliability over bright surfaces compared to dark water,
114 which is significant for our analysis (Garay et al., 2018).

115 2.2 MODIS

116 The Moderate Resolution Imaging Spectroradiometer (MODIS) is a payload instrument on
117 board the Terra and Aqua satellites. Terra's and Aqua orbit around the Earth from North to
118 South and South to North across the equator during the morning and afternoon respectively
119 (Kaufman et al., 1997). Terra MODIS and Aqua MODIS provides nearly daily coverage of
120 the Earth's surface and atmosphere in 36 wavelength bands, ranging from 0.412 to 41.2 μm ,
121 with spatial resolutions of 250 m (bands 1-2), 500 m (bands 3-7), 1000 m (bands 8-36).
122 Located near-polar orbit (705 km), MODIS has swath dimensions of 2330 km \times 10 km and
123 a scan rate of 20.3 rpm. With its high radiometric sensitivity and swath resolution MODIS
124 retrievals provides information about aerosols optical and physical characteristics. MODIS
125 uses 14 spectral band radiance values to evaluate atmospheric contamination and determine
126 whether scenes are affected by cloud shadow (Ackerman et al., 1998).

127 The Deep Blue is a NASA developed algorithm to calculate AOD over land using MODIS
128 data. By measuring contrast between aerosols and surface features, Deep Blue retrieves
129 AOD. Over bright land, Deep Blue uses (0.412, 0.470/0.490 μm) and dark land (0.470/0.490,
130 0.650 μm) for AOD retrievals. Over water, the Deep Blue algorithm is not used.

131 The MODIS dark-target algorithm derives aerosol characteristics, including AOD, over
132 ocean (dark in visible and longer wavelengths) and dark land surfaces (low values of surface
133 reflectance) (e.g., dark soil and vegetated regions) in parts of the visible (VIS, 0.47 and 0.65
134 μm) and shortwave infrared (SWIR, 2.1 μm) spectrum (Kaufman et al., 1997).

Deleted: is designed aerosol retrieval from MODIS observations

Deleted: ,

Deleted:

139
140 Level 2 collection 6.1 of the algorithm are used to retrieve MODIS aerosols' time series
141 data. Levy *et al.* (2010) reported that the dark-target algorithm AOD at 550 nm
142 measurement for (C005) includes uncertainty of $\pm (0.05\tau+0.03)$ and $\pm (0.15\tau+0.05)$ over
143 ocean and land respectively. This uncertainty is caused by uncertainties in computing cloud
144 masking, surface reflectance, aerosol model type (e.g., single scattering albedo), pixels
145 selections and instrument calibration. Both dark target and deep blue algorithms have been
146 used. Dark target retrievals were used over water regions while deep blue data were used
147 over land. Data are available at <https://giovanni.gsfc.nasa.gov/giovanni>. For regions like
148 Bahrain where large water body surrounds land, a combined Dark Target and Deep Blue
149 AOD for land and Ocean has been applied.

150 2.3 AERONET

151 The Aerosol Robotic Network (AERONET) [Holben et al., 1998](#) and [Holben et al., 2001](#) is a
152 ground-based remote sensing aerosols network that provides a long-term data related to
153 aerosol optical, microphysical and radiative properties. With over 700 global stations, the
154 AERONET data is widely used in validating satellite retrievals [Chu et al., 1998](#) and [Higurashi](#)
155 [et al., 2000](#).

156 The sun photometers used by AERONET, include sun collimators to measure spectral direct-
157 beam solar radiation, The collimators are used to determine columnar spectral AOD and
158 water vapour, provided at a temporal resolution of approximately 10–15 min ([Sayer et al.](#)
159 [2014](#)). AERONET direct-sun AOD has a typical uncertainty of 0.01–0.02 ([Holben et al.](#),
160 [1998](#)) and is provided at multiple wavelengths at 340, 380, 440, 500, 675, 950, and 1020 nm.
161 Seven AERONET sites were selected for MODIS/ Terra, MODIS/ Aqua, and MISR/Terra
162 satellites validation in this study (Table 1.). The sites were selected based on their geographic
163 locations to represent aerosols characteristics over North Africa and the Middle East (Farahat

Deleted: ¶

Deleted: measure spectral direct-beam solar radiation, as well as directional diffuse radiation in the solar almucantar

Deleted: .

Deleted: former are

Deleted: vapour

170 et al., 2016). A record of long-term data collection was another factor in the selection process.

171 Level 2.0 Version 3 AERONET data available at <https://aeronet.gsfc.nasa.gov> have been
172 used in the study.

173 Data Matching Approach

174 Multi-sensors data matching approach requires using only spatial and temporal matching data
175 to reduce uncertainties associated with using different instruments and clouds, shadow Liu
176 and Mishchenko (2008) and Mishchenko et al., 2009.

177 The comparison of MISR and MODIS products against AERONET is performed to evaluate
178 satellites' retrieval over individual North Africa and Middle East sites (see Table 1). There
179 is only a small number of AERONET measurements that are perfectly collocated with
180 MODIS and MISR. One way to work with this lack of compatibility problem is to compare
181 satellites measurements nearby a certain AERONET site and comparing AERONET
182 measurements nearly synchronized with the satellite overpass time (Sioris et al. 2017).
183 Another reasonable strategy is to average all satellite measurements with a certain distance
184 of an AERONET location and average all AERONET measurements within a certain time
185 range (Mishchenko et al., 2010). The results presented in this paper are based on the second
186 approach as it compares average spatial satellite measurements with average temporal
187 AERONET measurements. We implemented (Basart et al., 2009) approach in using a spatial
188 and temporal threshold of 50 km and 30 min for MISR, MODIS, and AERONET data
189 matching.

190 We use the Giovanni Multi-sensor Aerosol Products Sampling System MAPSS
191 (<http://giovanni.gsfc.nasa.gov/aerostat/>) for the data inter-comparison as aerosols products
192 are averaged from measurements that are within a radius of ~ 27.5 km from the AERONET
193 station and within 30 min of each satellite flyover over this location. These data are
194 represented in the article by MISR / MODIS “matched AERONET data”.

- Deleted: compatible
- Deleted: eliminate
- Deleted: shadow
- Deleted: and spatial and temporal retrievals produced by different instruments

200 “All data” represents AOD products at the selected station. AERONET station ‘all data’
 201 are obtained through AEROSOL ROBOTIC NETWORK (AERONET) website
 202 (<https://aeronet.gsfc.nasa.gov/>). Daily AOD data with level 2.0 quality was used in the
 203 analysis (Smirnov et al., 2000) . Level 2.0 AOD retrievals are accurate up to 0.02 for mid-
 204 visible wavelengths.
 205 MISR ‘all data’ is available through MISR website ([https://www-
 206 misr.jpl.nasa.gov/getData/accessData/](https://www-misr.jpl.nasa.gov/getData/accessData/)).
 207

208 3. Statistics

209 We have used two statistical parameters to compare data retrievals from space-borne and
 210 ground based sensors including:

211 (1) Correlation coefficient (R),

212 The correlation coefficient is a parameter to measure data dependence. If the value of R is
 213 close to zero, it indicates weak data agreement. And values close to 1 or -1 indicate that data
 214 retrievals are positively or negatively linearly related (Cheng et al., 2012).
 215

216 (2) Good Fraction (Gfraction).

217 The G- fraction indicator uses a data confidence range defined by MISR and MODIS
 218 Bruegge et al., 1998 and Remer et al., 2005 over the land and ocean that combines absolute
 219 and relative criterion and weights data equally such that small abnormalities will not affect
 220 the inter-comparison statistics (Kahn et al., 2009). In this study, we use MODIS confidence
 221 range which defines data retrieval as “good” if the difference between MODIS and
 222 AERONET is less than

$$223 \Delta\tau = \pm 0.03 \pm 0.05\tau_{AER}, \text{ Over ocean,} \quad (1)$$

$$224 \Delta\tau = \pm 0.05 \pm 0.15\tau_{AER}, \text{ Over land.} \quad (2)$$

Deleted: -

226

227 where τ_{AER} is the optical depth retrieved using AERONET stations. The Gfraction is the
228 percentage of MODIS data retrievals that satisfies (Equations (1) and (2)) over ocean and
229 land respectively. Optical depth threshold over land (Equation (2)) is higher than over ocean
230 (Equation (1)) due to harder data retrievals and high data instability over land.

231 A good aspect of using data confidence range is excluding small fraction data outliers from
232 producing inexplicably large influence on comparison statistics by weighting all events
233 equally.

234

235 4. Results and discussion

236 4.1 Validating MISR and MODIS AOD retrievals against AERONET observations 237 over the Middle East and North Africa

238 Illustrated in Figures 2, 3 and Tables 2, 3 is a regression analysis of MISR and MODIS Terra
239 AOD products against AERONET AOD over the seven AERONET sites, shown in Table1,
240 from 2000 – 2015.

241 The correlation coefficient between MISR and AERONET AOD at region 1 is equal to or
242 above 0.85 except in Bahrain during DJF and JJA (Figure (2) and Table 2), which could be
243 attributed to lack of data and the impact of water surface reflectivity over Bahrain. Similar
244 correlation coefficient values were found in region 2 where MISR-AERONET AOD shows
245 less error than MODIS (Figures (2, 3) and Table 3). In general, MODIS-AERONET AOD
246 correlation coefficient is lower than those of MISR at all sites, except Mezaira, where MISR
247 and MODIS matched AERONET AOD correlation almost match. The lowest MODIS-
248 AERONET AOD correlation coefficient was found over Cairo but could be attributed to the
249 lack of data availability at this location (Figs 3e-h). Low values of MODIS-AERONET
250 correlation coefficient is also found over Saada, Taman, and Sedee Boker sites.

Deleted: -

Deleted: 1

Deleted: 2

254 Over all AERONET stations, the number of MODIS AERONET matched AODs are 4 to 8
255 times those of MISR which is expected from the MISR's sampling.

256 Comparisons show that the difference between MISR and MODIS retrievals at the selected
257 AERONET sites could be significant as expected from the MODIS Dark Target algorithm
258 performance over bright land surfaces [Kokhanovsky et al. \(2007\)](#).

259 High AOD values over regions 1 and 2 measured by both AERONET and satellites' sensors
260 indicate higher dust activities that peaks during May – Aug during dust storms season. Higher
261 AOD values recorded during SON over Cairo station could be caused by seasonal rice straw
262 burning by farmers in Cairo, an environmental phenomena known as Cairo Black cloud
263 [\(Marey et al. 2010\)](#). As shown in (Figure (3)), the daily variability in MODIS measurements
264 is larger than those of MISR at all the three regions. In general, MODIS tends to
265 underestimate the AOD values on low dust seasons (Figures (2, 3) and Tables 2, 3).

266 The MODIS underestimated AOD values is more noticeable over Bahrain. This could be
267 attributed to large water body surrounding Bahrain, which should affect surface reflectivity.
268 Moreover, water in the Arabian Gulf has been polluted in recent years [\(Afnan 2013\)](#), leading
269 to possible changes in watercolour and uncertainties in calculating surface reflectivity. The
270 patchy land surface or pixel grid contaminated by water body is the dominant error sources
271 for MODIS aerosol inversion over the land areas [\(He et al. 2010\)](#).

272 Compared to MODIS, MISR's outperform in retrieving AOD over region 1 including vast
273 highly reflecting desert areas can be attributed to its multispectral and multi-angular
274 coverage, which make MISR provides better viewing over a variety of landscapes.
275 Meanwhile, MISR retrieval also take into consideration aerosols' particles nonsphericity,
276 which could have significant effect on its AOD retrievals [\(von Hoyningen-Huen and Posse](#)
277 [1997\)](#). MISR's retrieval did not well perform over Cairo site due to lack of matched points
278 in most of the seasons (13 in DJF, 5 in MAM & JJA, and 4 in SON during 2000 - 2015).

279

280 **4.2 Trends of AOD MISR, MODIS, and AERONET retrievals over the Middle East**
281 **and North Africa**

282 Figure 4 shows time series of monthly mean AOD derived from MODIS/Aqua,
283 MODIS/Terra, MISR and AERONET over a) dust b) biomass and c) mixed dominated
284 aerosol regions. The satellite AOD trends are calculated from the data collocated with
285 AERONET observations.

286 Trends of aerosol loading from 2000 to 2005 are analysed by plotting fitting lines of monthly
287 mean AOD retrievals by MISR and MODIS/Terra and Aqua. The AOD retrieved by different
288 instrument shows different trends. MODIS/ Aqua and MISR AOD at Solar Village have
289 positive trends, while MODIS/ Terra AOD have negative trends along time series (Fig. 4a).

290 Terra depicts a negative correlation coefficient with time while Aqua shows a positive one.
291 Terra AOD decreases 0.0071/year, while Aqua increases 0.0015/year. Aqua have lower
292 correlation coefficient for AOD compared to Terra, which indicates Aqua performed more
293 stable during the study period. Discrepancy between Aqua and Terra retrievals could be

294 related to instrument calibration, or the difference in aerosol and cloud conditions from the
295 morning to the afternoon. Both MODIS Aqua and Terra are underestimating AOD at Solar
296 Village. MISR AOD trend shows a better agreement with Solar Village AERONET AOD as
297 compared to MODIS.

298 In order to understand whether the discrepancy temporal trend of Terra and Aqua is a result
299 of regional conditions or if it exists in all sites, we investigated Terra, Aqua, MISR, and
300 AERONET over other sites.

301 Both MODIS/Aqua and MODIS/Terra AOD show a stable trend over time at Mezaria site
302 (not shown in the figure) with a correlation coefficient of 0.11 and 0.04 respectively. Both
303 Terra and Aqua AOD increase 0.008 and 0.001/year, respectively. Aqua AOD over Bahrain

Deleted: MODIS-Aqua AODs differ from those of MODIS-Terra.

Deleted: ¶

Deleted: s

Deleted: MODIS/A

309 (not shown in the figure) show, less time trend stability compared to those at Solar Village
310 with a correlation where Terra AOD decreases 0.0027/year, while Aqua increases
311 0.0066/year. Although Solar Village, Mezaria, and Bahrain are all located in or next to a
312 desert region, the inconsistency between Terra and Aqua measurements is subject to the
313 regional conditions. For example, the large water body surrounding Bahrain could mean that
314 the great majority of the MODIS retrievals are from Dark Target algorithm. MODIS/Aqua,
315 MODIS/Terra, and MISR AODs depicts a positive trend over Cairo, however a 2 years of
316 available AERONET data is not sufficient for the trend analysis (Fig. 4b). Over Cairo,
317 MODIS/Terra, MODIS Aqua, and MISR measurements agree on AOD increase by 0.001,
318 0.0007, and 0.0007/year respectively with correlation coefficients 0.10, 0.04, and 0.22
319 respectively. Despite the deviation between the three aforementioned sensors, they all agree
320 on AOD temporal trend increase over Cairo. This could be attributed to the high pollution
321 level at the mega city of Cairo due to high population, vehicle emission, and biomass burning.
322 Taman site (Fig. 4c): MISR AOD agrees with Taman AERONET on a positive trend
323 indicating the efficiency of MISR V22 algorithm over green areas with less black carbon
324 particles. Aqua measurements show temporal AOD decrease of 0.0079/year with a
325 correlation coefficient of 0.81 and Terra show AOD decrease of 0.0043/year with a
326 correlation coefficient of 0.35. Meanwhile, MISR shows AOD increase of 0.0014/year with
327 a correlation coefficient of 0.19.
328 Long-range (2000 – 2015) tendency indicates that contradictory AOD trend of Terra and
329 Aqua is individually explicit for each site and does not necessarily apply everywhere.
330 AOD difference between Terra and Aqua could be used as another indicator of the long-
331 range satellites performance. AOD difference (Terra AOD minus Aqua AOD) varies from -
332 0.01 to 0.19, -0.10 to 0.18, -0.02 to 0.13 over Solar Village, Taman, and Cairo respectively
333 (Fig. 5). Over the Solar Village, Terra overestimates AODs during 2002-2004 and

Deleted: coefficient 0.63

Deleted: MODIS/Aqua, MODIS/ Terra,

Deleted: negative

Deleted: indicating data stability over this site

338 underestimates the AOD after 2005. Although Cairo and Taman show similar trend however
339 over/underestimation amount is not unique for all sites. This is an indication that Aqua and
340 Terra retrievals disagreement takes place regardless of the region but site sampling has
341 significant effect on the amount of contradiction.

342 Statistical comparison between MISR and MODIS/Terra AODs at corresponding

343 AERONET stations is performed by calculating Gfraction using of $\Delta\tau = \pm 0.05 \pm 0.15\tau_{AERO}$

344 as a confidence interval. Over the region 1, MISR AODs retrievals are more accurate than
345 MODIS retrievals. MODIS, however, perform better over region 2 sites with high percent of
346 the data points falling within the confidence range (Tables 2 and 3). High light reflections
347 from the desert landscape surrounding region 1 could have an effect on MODIS retrievals.

348 Excluding Bahrain and Cairo for low data retrievals the performance of MODIS tends to be
349 similar over all region with ~ 68 percent of AODs retrievals fall within the
350 $\Delta\tau = \pm 0.05 \pm 0.15\tau_{AERO}$ confidence range of the AERONET AOD while MISR retrievals
351 show better data performance with ~ 72 percent falls within the same confidence range. This
352 could be attributed to low number of retrievals available for Bahrain and Cairo compared to
353 other sites. Vast sea region surrounding Bahrain and complex landscape in Cairo could also
354 have an impact on retrievals.

355 **4.3 Evaluating the MISR and MODIS climatology over Middle East and North Africa**

356 Comparisons between MISR and MODIS AOD at selected AERONET stations over the
357 2000 – 2015 period are illustrated in Figures 6- 12.

358 Figure (6a, b) shows histogram of the MISR, MODIS and AERONET AOD at Solar Village
359 for MISR and MODIS data points collocated with AERONET observations. The mean,
360 standard deviation, and number of measurements are also presented.

361 MISR tends to underestimate the frequency of low AODs compared to AERONET but
362 overestimate the frequency of high AODs. MISR histograms show prominent peaks at 0.55

Deleted: -

364 and 0.75 not seen in AERONET. MISR and AERONET AOD climatology agree well with
365 one another. MODIS also tends to underestimate the frequency of low AOD events and
366 overestimate the frequency of high AOD events. High surface reflectance could cause
367 overestimation in MODIS AODs (Ichoku et al., 2005). Both MISR and MODIS provide a
368 good representation of the AOD climatology as compared to AERONET at the Solar Village.
369 Mezaria station, which is located at an arid region in the UAE, has a similar climatology to
370 the Solar Village site with dust dominating aerosol. Figure (7a, b) shows histogram of the
371 MISR, MODIS and AERONET AOD at Mezaria.

372 Unlike Solar Village, there is a big difference between the number of samples in the matched
373 data set and full AERONET climatology. For MISR there are 116 matched cases and for
374 MODIS there are 498 compared to the 1517 for the entire site. This has an impact on the
375 overall assessment showing significant differences between the matched data and the full
376 climatology for both MISR and MODIS. First, for the MISR case, the matched AERONET
377 data have the highest frequency at AODs of 0.3 and 0.35, but the climatology shows the
378 highest frequency at an AOD of 0.25. Second AODs in the range of 0.3 to 0.45 are
379 oversampled relative to the climatology, and AODs less than 0.3 and greater than 0.5 are
380 under-sampled with no AODs greater than 0.8. MODIS matched AERONET data show
381 prominent peaks at 0.3 and 0.4 compared to the climatology that has a single peak at 0.25.
382 Similar to MISR AODs are under-sampled less than 0.3 and greater than 0.6.

383 MISR AOD retrievals matched to AERONET capture the variability in the distribution, but
384 as in the case of Solar Village the frequency of low AOD events is underestimated and the
385 frequency of high AOD events is overestimated. However, MISR does capture events with
386 AODs greater than 1. A similar situation is seen in the MODIS comparison, but MODIS
387 appears to do a better job capturing the overall shape of the AERONET AOD histogram for
388 this site.

389 The Bahrain AERONET site is located in Manama fairly close to the Arabian Gulf, a location
390 very different from the previous two sites. The site is also located in an urban area suffers
391 from significant load of anthropogenic aerosols as a consequence of rapid Aluminium
392 industrial development (Farahat 2016). Figure (8a, b) shows histogram of the MISR, MODIS
393 and Bahrian AERONET measurements with statistical analysis displayed. The AERONET
394 data matched to MISR show significant peaks at 0.25, 0.35, and 0.5 not seen in the all data
395 climatology that has a single peak at 0.35. AODs less than 0.25 and greater than 0.6 are not
396 representative in the matched data set at all. MISR is representing the peaks at 0.25 and 0.35
397 in the matched data set but misses the peak at 0.5. Ångström exponent (AE), dependency of
398 the AOD on wavelength, can also be used to determine particles' size where the smaller the
399 particle the larger the exponent. AE analysis show that the first peak at 0.25 is indicative of
400 industrial particles with high AE values and the second peak at 0.35 indicates dust aerosol.
401 The MISR climatology agrees well with the AERONET all data climatology for all AODs.
402 MODIS on the other hand shows an extremely large frequency of AODs at 0.1 not
403 represented by AERONET coupled with an underestimation of AODs greater than 0.3. This
404 could be attributed to the size of the matching window and MODIS retrievals preferentially
405 coming from the Arabian Gulf.
406 SAADA station is located close to some hiking trails at the Agoundis Valley in the Atlas
407 Mountains about 197 km from the city of Marrakesh.
408 MISR AODs matched to AERONET agree well with MISR full climatology retrievals over
409 SAADA station. Both retrievals slightly underestimate SAADA full climatology and over
410 estimates SAADA matched data retrievals at AODs equal to 0.1 while show good agreement
411 for AODs greater than 0.1. MODIS matched to AERONET retrievals overestimate the
412 frequency of AODs greater than 0.3. While MODIS AODs matched to AERONET captures
413 climatology at AODs between 0.2 to 0.25, AODs frequency retrievals are under-sampled at

414 AODs between 0.1 to 0.15 with about 13 % less events than SAADA all data retrievals at
415 AODs equal to 0.1.

416 Figure (9a, b) indicates right skewed distribution of SAADA AODs towards small AOD
417 values with 11.5 % and 30.1 % of AODs > 0.4 as measured by MISR and MODIS
418 respectively. Taking into consideration MODIS overestimation we conclude that SAADA
419 site is characterized by small AODs values and this could be related to the land topography
420 where the station is located.

Deleted: topology

421 While MISR is capturing high AODs climatology over SAADA, both MISR and MODIS
422 are underestimating the frequency of lower AODs events. Nevertheless, MISR captures the
423 climatology of AODs less than 0.1 missed by MODIS retrievals.

424 Taman AERONET station is located at the oasis city of Tamanrasset, which lies in Ahaggar
425 National Park at southern Algeria.

426 Figure (10 a, b) depicts that Taman AERONET AOD climatology is similar to those at
427 SAADA and has a high frequency of low AODs events. Both MISR AODs matched to
428 AERONET and MISR all data do not well capture the frequency of AODs less than 0.1 or
429 larger than 1 while well describe the climatology for AODs in the range of 0.1 to 1. MODIS
430 AODs matched data to AERONET correctly describe climatology with slight overestimation
431 of AODs frequencies between 0.05 – 0.15 while not capturing AODs frequencies greater
432 than 1. MISR and MODIS show similar prominent peaks at 0.1, 0.25, and 0.35, not observed
433 in Taman AERONET AOD climatology, with more peaks observed by MISR at 0.5, 0.6, and
434 0.8. Average AODs in SAADA and Taman is ~ 50 percent less than observed at Solar
435 Village, Mezaria, and Bahrain sites.

436 Except for AODs greater than 1 where ground observations could be more robust, both MISR
437 and MODIS retrievals can provide very good climatology matching over Taman site.

439 Taking into consideration lower number of MISR matching AERONET observations
440 compared to MODIS ~ 33 and 43 percent over SAADA and Taman respectively, MISR is
441 outperforming over these two sites, which can be attributed to its multiangle viewing
442 capabilities over complex terrains including mountainous areas (Atlas Mountains).
443 Cairo is a mega city well known for its high pollution due to traffic and agriculture activities.
444 MISR and MODIS matched data correctly capture AOD climatology over Cairo compared
445 to AERONET as shown in Figure (11a, b). MISR retrievals collocated with AERONET
446 capture prominent peaks of AERONET AOD at 0.15 – 0.25 and 0.5 with small
447 underestimation observed at 0.3. MISR ‘all data’ AOD climatology over Cairo station agrees
448 better with AERONET AOD climatology vs. collocated dataset with some oversampling at
449 0.15. Frequency of high AODs retrievals at 0.7 and 0.8 have not been captured by MISR
450 matched or all data retrievals. MODIS matched to AERONET AODs are also able to well
451 present Cairo climatology data with a high overestimation of AODs frequency between 0.05
452 - 0.2 and an underestimation of AODs larger than 0.4.
453 The complex landscape and home-grown emissions in Cairo could impose major challenges
454 in MODIS AODs retrievals. Moreover, Cairo is one of the most densely populated cities in
455 the world that hosts major commercial and industrial centers in North Africa. Cairo also has
456 complicated aerosols structure developed by long range transported dust in the spring,
457 biomass burning in the fall, strong traffic and industrial emissions (Marey et al., 2010).
458 Over Cairo station, MODIS correctly represents ground observations for AODs between 0.2
459 - 0.4 while MISR all data better represents AOD climatology for AODs greater than 0.4.
460 There is not enough collocated MISR-AERONET AODs to evaluate MISR ‘matched AOD’
461 climatology.
462 MISR, MODIS climatology at SEDEE Boker are illustrated in Figures (12a, b).

Deleted:

464 MISR 'matched' AODs frequency show significant underestimation for AODs less than 0.2
465 and an overestimation between 0.2 – 0.4 compared with AERONET retrievals. MISR
466 correctly captures the climatology for AODs events greater than 0.4. MISR 'matched' and
467 'all data' retrievals peaks at 0.25 and 0.2 respectively producing high frequency of AODs
468 oversampling compared to AERONET. MISR data retrievals do not capture the climatology
469 for AODs less than 0.1 over this site coincident with what was previously observed over
470 other sites. MODIS matched AERONET data underestimates frequency of AODs less than
471 0.2 while overestimates the frequencies between 0.2 - 0.6, and well match frequencies of
472 higher AODs events larger than 0.6. MODIS retrievals are characterized by two prominent
473 peaks at 0.1 and 0.25 that are not found in the AERONET matched data.

474 At Sedee, MISR and MODIS retrievals are better in matching frequency of high AODs
475 retrievals (greater than 0.4) than the frequency of low AODs. This could be an effect of
476 possible long-range transport to Sedee Boker site (Farahat et al. 2016) along with complex
477 mixtures of dust, pollution, smoke, and sea salt that could result in uncertainties in MISR and
478 MODIS aerosol model selection.

479 In the summary, MISR tends to underestimate AODs > 0.4 over Solar Village, Mezarria,
480 Bahrain, and Cairo while agrees with AERONET over SAADA, Taman and Sedee Boker at
481 all ranges of AODs. This could be expounded by insufficient particle absorption in MISR
482 V22 algorithm (Kahn et al., 2005). Spherical particle absorption is produced by externally
483 mixing small black carbon particles.

484 Percentage of MISR, MODIS, and AERONET AODs greater than 0.4 recorded is shown in
485 Table 4. Over Solar Village, both MISR and MODIS well capture high AODs greater than
486 0.4 with very good agreement with the ground observations. Over Mezarria, both MISR and
487 MODIS are over estimating the percentage of AODs greater than 0.4 by about 15.5 and 10.5
488 percent respectively. MISR all data agrees well with AERONET all data in representing high

489 AOD over Bahrain while MODIS shows significant under-representation of those events by
490 about 15 percent, less than reported by Bahrain AERONET station. At SAADA, MISR AOD
491 agrees with AERONET in showing low percentage of AODs greater than 0.4, while MODIS
492 retrievals overestimate percentage by about 24 percent. MISR AOD over Taman AERONET
493 station shows very good agreement, while MODIS is slightly overestimating AODs. Among
494 all seven sites considered in this study, Sedee Boker shows lowest occurrence of AODs
495 greater than 0.4, which is confirmed by both MISR and MODIS retrievals. Cairo AERONET
496 records the highest frequency of AODs > 0.4, however this is largely underestimated by both
497 MISR and MODIS retrievals.

498 It can concluded from the previous discussion that atmosphere around SAADA, Taman,
499 and Sedee Boker sites is relatively clean and aerosol loads are small compared to Solar
500 Village, Mezaria, Bahrain, and Cairo, however this could be affected by the location where
501 AERONET station is installed for example SAADA and Taman stations are installed in a
502 remote mountainous region away from urbanization while Cairo station is installed in the
503 middle of large residential region with significant local emissions.

504

505 **Conclusion**

506 The performance of MODIS, MISR retrievals with corresponding AERONET
507 measurements over different geographic locations in the Middle East and North Africa was
508 investigated during 2000 – 2015.

509 Long-range observations show dissimilar AODs trends between MODIS/Aqua,
510 MODIS/Terra, MISR and AERONET measurements. MODIS/Aqua matched AERONET
511 retrievals show stable trend over all sites while, MODIS/Terra matched AERONET retrievals
512 show significant downward trend indicating possible changes in the sensor performance.

513 MISR matched AERONET AODs data depict high correlation compared to
514 AERONET indicating good agreement with ground observations with about 72 percent of
515 AODs retrievals fall within the expected confidence range.

516 Consistency of MODIS and AERONET AODs vary based on the season, study area,
517 and dominant aerosols type with about 68 percent of the retrieved AODs values fall within
518 expected confidence range with the lowest performance over mixed particles regions.

519 Comparing satellites' AODs retrievals with corresponding AERONET
520 measurements show that space-borne data retrievals accuracy can be affected by landscape,
521 topology, and AOD range at which data is retrieved.

522 Few AERONET sites are verified where MISR and MODIS retrievals well agree with
523 ground observations, where other sites only MISR or MODIS could correctly describe the
524 climatology.

525 The AODs range at which MISR or MODIS could correctly describe ground
526 observation is also investigated over different AERONET sites. Over Solar Village both
527 MISR and MODIS tend to underestimate the frequency of low AODs and overestimate the
528 frequency of high AODs compared to AERONET with MISR histograms show prominent
529 peaks at 0.55 and 0.75 not shown in AERONET. MISR can capture the frequency of AODs
530 greater than 1 mostly missed by MODIS. Both MISR and MODIS are found to provide good
531 representation of the AOD climatology over the Solar Village site.

532 Similar to Solar Village, MISR underestimates frequency of lower AODs and
533 overestimate frequencies of high AODs over Mezaria. MISR is able to correctly capture the
534 frequency of AODs greater than 1, while MODIS retrievals are found to better represent the
535 overall climatology. This is due to low number of MISR – matched AERONET retrievals
536 compared to MODIS over this site. Prominent peaks at 0.3 and 0.4 were observed in MODIS
537 matched Mezaria retrievals compared to the climatology, which has a single peak at 0.25.

538 Large water body surrounding Bahrain makes MODIS data preferentially comes from
539 the Arabian Gulf which produces an extremely large frequency of AODs at 0.1 not observed
540 in AERONET measurements paired with an underestimation of AODs greater than 0.3.
541 Meanwhile, MISR retrievals agree well with AODs climatology over Bahrain.
542 MISR AODs retrievals slightly underestimate SAADA climatology while show good
543 agreement for AODs greater than 0.1. MODIS retrievals underestimate the frequency of
544 AODs retrievals between 0.1 to 0.15, match climatology at AODs between 0.2 to 0.25, and
545 overestimate the frequency of AODs greater than 0.3. SAADA site is characterized by small
546 frequency of low AODs values and this could be related to the landscape nature surrounding
547 Saada station. MISR is found be outperforming over Saada and Taman stations which can be
548 attributed to its viewing multispectral and multiangular capabilities over mountainous
549 regions.

550 MISR retrievals well capture prominent peaks of AERONET data at 0.15 to 0.25 and
551 0.5 with small underestimation observed at 0.3 over Cairo. It is recommended to use MISR
552 all data rather than matched data only over Cairo as it is found to do a better job in describing
553 the climatology over this station. MODIS data retrievals are also able to well present Cairo
554 climatology with a high overestimation of AODs frequency between 0.05 to 0.2 and an
555 underestimation of AODs larger than 0.4. While both MISR and MODIS well describe
556 climatology over Cairo station, MODIS can correctly represent ground observations between
557 0.2 to 0.4.

558 Over Sedee Boker both MISR and MODIS retrievals well describe the climatology however
559 they are more successful in matching frequency of high AODs greater than 0.4.

560 Based on analysing frequency of AODs greater than 0.4, it was found that Saada, Taman,
561 and Sedee Boker are having better air quality compared to other sites while Cairo was found
562 to be the most polluted site.

563 Results presented in this study are important in providing a guideline for satellites retrievals
564 end users on which sensor could provide reliable data over certain geographic location and
565 AOD range.

566 Adjacent geographic location and local climate among sites does not always
567 guarantee that same sensor will provide consistent retrievals over all sites. For example, Solar
568 Village, and Bahrain AERONET are surrounded by large desert regions in the and sharing
569 almost similar climatic conditions, but MODIS is found to be more successful in describing
570 climatology over Solar Village than over Bahrain and this could be attributed to different
571 factors related to surface reflection, cloud coverage, and the large water body surrounding
572 Bahrain. Thus in order to decrease data uncertainty, it is important to determine which sensor
573 provides best retrieval over certain geographic location and AOD range.

574

575 **Acknowledgements**

576 The authors would like to acknowledge the support provided by the Deanship of Scientific
577 Research (DSR) at the King Fahd University of Petroleum and Minerals (KFUPM) for
578 funding this work through project # IN161053. Portions of this work were performed at the
579 Jet Propulsion Laboratory (JPL), California Institute of Technology, under a contract with
580 the National Aeronautics and Space Administration. The author would like to thank Michael
581 Garay (MJG) and Olga Kalashnikova (OVK) (JPL) for their suggestion of investigating
582 satellites – AERONET matched data climatology, and discussion during the data analysis.
583 The author would also like to thank Hesham El-Askary (Chapman University) for providing
584 recommendation about AERONET data over North Africa and the Middle East as well as
585 reviewing the English in the manuscript. We thank the MISR project for providing facilities,
586 and supporting contributions of MJG and OVK. Finally, we thank the reviewers for
587 suggestions, which improved the manuscript.

588

589

590 **Author Contributions:** Ashraf Farahat analysed the data, performed the statistical analysis
591 and wrote the manuscript.

592

593 **Conflicts of Interest:** The authors declare no conflict of interest.

594

595
596
597
598
599

References

- 600 1. Abdi, V., Flamant, C., Cuesta, J., Oolman, L., Flamant, P., and Khaledifard, H. R.
601 Dust transport over Iraq and northwest Iran associated with winter Shamal: A case
602 study. *J. Geophys. Res.*, 117, D03201, 2013.
- 603
604 2. Ackerman, S., Strabala, K. I., Menzel, W. P., Frey, R. A., Moeller, C. C. and Gumley,
605 L. E. (1998): Discriminating clear sky from clouds with MODIS. *J. Geophys. Res.*,
606 103, 32 141–157, 1998.
- 607
608 3. Afnan, F. Heavy metal, trace element and petroleum hydrocarbon pollution in the
609 Arabian Gulf: Review, *Journal of the Association of Arab Universities for Basic and
610 Applied Sciences*, 17, 90-100, 2015.
- 611
612 4. Ansmann, A., Petzold, A., Kandler, K., Tegen, I., Wendisch, M., Müller, D.,
613 Weinzierl, B., Müller, T., and Heintzenberg, J. Saharan Mineral Dust Experiments
614 SAMUM-1 and SAMUM-2: what have we learned? *Tellus B*, 63, 403–429, 2011.
- 615
616 5. Basart, S., Pérez, C., Cuevas, E., Baldasano, J. M., and Gobbi, G. P. Aerosol
617 characterization in Northern Africa, Northeastern Atlantic, Mediterranean Basin and
618 Middle East from direct-sun AERONET observations. *Atmos. Chem. Phys.*, 9, 8265-
619 8282, 2009.
- 620
621 6. Böer B., An introduction to the climate of the United Arab Emirates (review). *J*
622 *Arid Environ.*, 35:3–16, 1997.
- 623
624 7. Bou Karam, D., Flamant, C., Cuesta, J., Pelon, J., and Williams, E. Dust emission
625 and transport associated with a Saharan depression: February 2007 case, *J.*
626 *Geophys. Res.*, 115, D00H27, 2010.
- 627
628 8. Bre´on, F-M., Vermeulen, A., Descloitres, J. An evaluation of satellite aerosol
629 products against sunphotometer measurements. *Remote Sensing Environ.*, 115,
630 3102–11, 2011.
- 631
632 9. Bruegge, C., Chrien, N., Kahn, R., Martonchik, J., and Diner, D. MISR radiometric
633 uncertainty analyses and their utilization within geophysical retrievals. *IEEE Trans.*
634 *Geosci. Remote Sens.*, 36, 1186- 1198, 1998.
- 635
636
637 10. Chin, M., Diehl, T., Tan, Q., Prospero, J. M., Kahn, R. A., Remer, L. A., Yu, H.,
638 Sayer, A. M., Bian, H., Geogdzhayev, I. V., Holben, B. N., Howell, S. G.,
639 Huebert, B. J., Hsu, N. C., Kim, D., Kucsera, T. L., Levy, R. C.,

- 640 Mishchenko, M. I., Pan, X., Quinn, P. K., Schuster, G. L., Streets, D. G.,
 641 Strode, S. A., Torres, O., and Zhao, X.-P. Multi-decadal aerosol variations from
 642 1980 to 2009: a perspective from observations and a global model, *Atmos. Chem.*
 643 *Phys.*, 14, 3657-3690, 2014.
- 644
- 645 11. Chu, D. A., Kaufman, Y. J., Remer, L. A., and Holben, B. N. Remote sensing of
 646 smoke from MODIS airborne simulator during the SCAR-B experiment. *J. Geophys.*
 647 *Res.*, 103, 31, 979– 987, 1998.
- 648
- 649 12. Derimian, Y., Karnieli, A., Kaufman, Y. J., Andreae, M. O., Andreae, T. W.,
 650 Dubovik, O., Maenhaut, W., Koren, I., and Holben, B. N. Dust and pollution
 651 aerosols over the Negev desert, Israel: Properties, transport, and radiative effect. *J.*
 652 *Geophys. Res.*, 111, D05205, 2006.
- 653
- 654 13. Dubovik, O. and King, M. D. A flexible inversion algorithm for retrieval of aerosol
 655 optical properties from Sun and sky radiance measurements. *J. Geophys. Res.*, 105
 656 206730–20696, 2000.
- 657
- 658 14. Dubovik, O., Holben, B. N., Eck, T. F., Smirnov, A., Kaufman, Y. J., King, M. D.
 659 Tanre, D., and Slutsker, I. Variability of absorption and optical properties of key
 660 aerosol types observed in worldwide locations. *J. Atmos. Sci.*, 59, 590–608, 2002.
- 661
- 662 15. Dubovik, O., Sinyuk, A., Lapyonok, T., Holben, B., Mishchenko, M., Yang, P., Eck,
 663 T., Volten, H., Muñoz, O., Veihelmann, B., van der Zande, W. J., Leon, J.-F.,
 664 Sorokin, M., and Slutsker, I. The application of spheroid models to account for
 665 aerosol particle non-sphericity in remote sensing of desert dust. *J. Geophys. Res.*,
 666 111, D11208, 2006.
- 667
- 668 16. Eck, T., Holben, B. N., Reid, J. S., O'Neill, N. T., Schafer, J. S., Dubovik, O.,
 669 Smirnov, A., Yamasoe, M. A., and Artaxo, P. High aerosol optical depth biomass
 670 burning events: A comparison of optical properties for different source regions,
 671 *Geophys. Res. Lett.*, 200b, 30, 20, 2035, 2003b.
- 672
- 673 17. Eck, T., et al. Climatological aspects of the optical properties of fine/coarse mode
 674 aerosol mixtures. *J. Geophys. Res.*, 115, D19205, 2010.
- 675
- 676 18. Elagib, N., Addin Abdu A. Climate variability and aridity in Bahrain. *J. Arid*
 677 *Environ.*, 36:405–419, 1997.
- 678
- 679 19. El-Askary H., Farouk R., Ichoku C., and Kafatos M. Inter-continental transport of
 680 dust and pollution aerosols across Alexandria, Egypt, *Annales Geophysicae*, 27,
 681 2869–2879, 2009.
- 682
- 683 20. Farahat, A., El-Askary, H., and Al-Shaibani, A. Study of Aerosols' Characteristics
 684 and Dynamics over the Kingdom of Saudi Arabia using a Multi Sensor Approach
 685 Combined with Ground Observations. *Advances in Meteorology*, Article ID
 686 247531, 2015.
- 687

- 688 21. Farahat, A. Air Pollution in Arabian Peninsula (Saudi Arabia, United Arab
689 Emirates, Kuwait, Qatar, Bahrain, and Oman): Causes, Effects and Aerosol
690 Categorization. Arab J of Geosci., 9, 196, 2016.
691
- 692 22. Farahat, A., El-Askary, H., and Dogan, A. U., 2016: Aerosols size distribution
693 characteristics and role of precipitation during dust storm formation over Saudi
694 Arabia. Aerosol Air Qual. Res., 16, 2523-2534, 2016.
695
- 696 23. Farahat, A., El-Askary, H., Adetokunbo, P., Abu-Tharr, F. Analysis of aerosol
697 absorption properties and transport over North Africa and the Middle East using
698 AERONET data. Annales Geophysicae., 34:11, 1031-1044, 2016.
699
- 700 24. He, Q., Li, C., Tang, X., Li, H., Geng, F., Wu, Y. Validation of MODIS derived
701 aerosol optical depth over the Yangtze River Delta in China. Remote Sensing
702 Environ., 114, w21649–61, 2010.
- 703
- 704 25. Higurashi, A., and Nakjima, T. Development of a two-channel aerosol retrieval
705 algorithm on a global scale using NOAA AVHRR. J. Atmos. Sci., 56, 924–941,
706 1999.
- 707
- 708 26. Holben, B., Eck, T., Slutsker, I., Tanre, D., Buis, J., Setzer, A. et al. AERONET—
709 A federated instrument network and data archive for aerosol characterization.
710 Remote Sensing Environ., 66, 1–16, 1998.
711
- 712 27. Holben, B., Smirnov, A., Eck, T., Slutsker, I., Abuhassan, N., Newcomb, W., et al.
713 An emerging ground-based aerosol climatology—Aerosol optical depth from
714 AERONET, J. Geophys Res., 106, 12067–97, 2001.
715
- 716 28. Hoell, A., Funk, C., and Barlow, M. The regional forcing of Northern Hemisphere
717 drought during recent warm tropical west Pacific Ocean La Niña events. Clim.
718 Dyn., 42, 3289–3311, 2013.
719
- 720
- 721 29. Hsu, N., Gautam, R., Sayer, A., Bettenhausen, C., Li, C., Jeong, M., Tsay, S., and
722 Holben, B. Global and regional trends of aerosol optical depth over land and ocean
723 using SeaWiFS measurements from 1997 to 2012. Atmos. Chem. Phys., 12, 8037–
724 8053, 2012.
725
- 726 30. Ichoku, C., Chu, D. A., Mattoo, S., Kaufman, Y. J., Remer, L. A., Tanre, D.,
727 Slutsker, I., and Holben, B. N. A spatio-temporal approach for global validation
728 and analysis of MODIS aerosol product, Geophys. Res. Lett., 29, 12, 8006, 2002.
729
- 730 31. [Garay, M., Kahn, R., Bull, M., Nastan, A., Witek, M., Seidel, F., Diner, D.,
731 Limbacher, J., Kalashnikova, O., Data Quality Statement for the MISR Level 2
732 Aerosol Product, Jet Propulsion Laboratory, California Institute of Technology,
733 2018](#)
734

Formatted: Font: (Default) +Headings CS (Times New Roman), 12 pt, Complex Script Font: +Headings CS (Times New Roman), 12 pt

Formatted: Indent: Before: 0.5", Line spacing: Multiple 1.08 li, No bullets or numbering, Adjust space between Latin and Asian text, Adjust space between Asian text and numbers, Tab stops: Not at 0.63"

- 735 32. Ginoux, P., Chin, M., Tegen, I., Prospero, J., Holben, B., Dubovik, O., and Lin, S.-
736 J. Sources and global distributions of dust aerosols simulated with the GOCART
737 model, *J. Geophys. Res.*, 106, 20255 – 20273, 2001.
738
- 739 33. Kahn, R. A., Gaitley, B. J., Martonchik, J. V., Diner, D. J., Crean, K. A. and Holben,
740 B. Multiangle ImagingSpectroradiometer (MISR) global aerosol optical depth
741 validation based on 2 years of coincident Aerosol Robotic Network (AERONET)
742 observations, *J. Geophys. Res.*, 110, 2005.
743
- 744 34. Kahn, R., Garay, M., Nelson, D., Yau, K., Bull, M., Gaitley, B. et al. Satellite-
745 derived aerosol optical depth over dark water from MISR and MODIS:
746 Comparisons with AERONET and implications for climatological studies. *J.*
747 *Geophys. Res.*, 112, D18205, 2007.
748
- 749 35. Kahn, R., Nelson, D., Garay, M., Levy, R., Bull, M., Diner, D., et al. MISR aerosol
750 product attributes, and statistical comparisons with MODIS. *IEEE Trans Geosci*
751 *Remote Sensing*, 47, 4095–114, 2009.
752
- 753 36. Kim, D., Chin, M., Bian, H., Tan, Q., Brown, M. E., Zheng, T., You, R., Diehl, T.,
754 Ginoux, P., and Kucsera, T. The effect of the dynamic surface bareness on dust
755 source function, emission, and distribution, *J. Geophys. Res.*, 118, 1–16, 2013.
756
- 757 37. Kaufman, Y., Tanre, D., Remer, L., Vermote, E., Chu, A., and Holben, B.
758 Operational remote sensing of tropospheric aerosol over land from EOS moderate
759 resolution imaging spectroradiometer. *J. Geophys. Res.-Atmos.*, 102, D14, 17051–
760 17067, 1997.
761
- 762 38. Kokhanovsky, A., Breon, F., Cacciari, A., Carboni, E., Diner, D., Di Nicolantonio,
763 W. et al. Aerosol remote sensing over land: a comparison of satellite retrievals using
764 different algorithms and instruments. *Atmos Res.*, 85, 372–94, 2007.
765
- 766 39. Liu, L., Mishchenko, M. Toward unified satellite climatology of aerosol properties:
767 direct comparisons of advanced level 2 aerosol products. *JQSRT.*, 109, 2376–85,
768 2008.
769
- 770 40. Marey, H., Gille, J., El-Askary, H., Shalaby, E. , and El- Raey, M. Study of the
771 formation of the “black cloud and its dynamics over Cairo, Egypt, using MODIS
772 and MISR sensors. *J. Geophys. Res.*, 115, D21206, 2010.
773
- 774 41. Martonchik, J., Diner, D., Crean, K., and Bull, M. Regional aerosol retrieval results
775 from MISR. *IEEE Trans. Geosci. Remote Sens.*, 40, 1,520–1,531, 2002.
776
- 777 42. Mishchenko, M., I. Geogdzhayev, L. Liu, A. Lacis, B. Cairns, L. Travis. Toward
778 unified satellite climatology of aerosol properties: what do fully compatible
779 MODIS and MISR aerosol pixels tell us? *J Quant Spectrosc Radiat Transfer.* 110,
780 402–8, 2009.
781
- 782 43. Mishchenko, M., Liu, L., Geogdzhayev, I., Travis, L., Cairns, B., Lacis, A. Toward
783 unified satellite climatology of aerosol properties: 3. MODIS versus MISR versus
784 AERONET. *J Quant Spectrosc Radiat Transfer.*, 111, 540–52, 2010.

- 785
786
787
788
789
790
791
792
793
794
795
796
797
798
799
800
801
802
803
804
805
806
807
808
809
810
811
812
813
814
815
816
817
818
819
820
821
822
823
824
825
826
827
828
829
830
831
832
833
44. Remer, L., Kaufman, Y., Tanre', D., Mattoo, S., Chu, D., Martins, J., et al. The MODIS aerosol algorithm, products, and validation. *J Atmos Sci.*, 62, 947–73, 2005.
 45. Sadiq, M. and McCain, J. *The Gulf War Aftermath: An Environmental Tragedy.*, 1st ed., Springer, 1993.
 46. Sayer, A., Hsu, N., Eck, T., Smirnov, A., and Holben, B. AERONET-based models of smoke-dominated aerosol near source regions and transported over oceans, and implications for satellite retrievals of aerosol optical depth. *Atmos. Chem. Phys.*, 14, 11493-11523, 2014.
 47. Schepanski, K., Mallet, M., Heinold, B., and Ulrich, M.: North African dust transport toward the western Mediterranean basin: atmospheric controls on dust source activation and transport pathways during June–July 2013, *Atmos. Chem. Phys.*, 16, 14147-14168, 2016.
 48. Sioris, C. E., McLinden, C. A., Shephard, M. W., Fioletov, V. E., and Abboud, I.: Assessment of the aerosol optical depths measured by satellite-based passive remote sensors in the Alberta oil sands region, *Atmos. Chem. Phys.*, 1931-1943, 2017.
 49. Smirnov, A., Holben, B., Eck, T., Dubovik, O., and Slutsker, I. Cloud-screening and quality control algorithms for the AERONET data-base, *Remote Sens. Environ.*, 73, 337 – 349, 2000.
 50. Solomos, S., Ansmann, A., Mamouri, R.-E., Biniotoglou, I., Patlakas, P., Marinou, E., and Amiridis, V. Remote sensing and modelling analysis of the extreme dust storm hitting the Middle East and eastern Mediterranean in September 2015, *Atmos. Chem. Phys.*, 17, 4063-4079, 2017.
 51. Todd M., R. Washington, Vanderlei, M., Dubovik, O., Lizcano, G., M'Bainayel, S., Engelstaedter, S. Mineral dust emission from the Bodélé Depression, northern Chad, during BoDEx 2005. *J. Geophys. Res.*, 112. D06207, 2007.
 52. Von Hoyningen-Huene, W., Posse, P. Nonsphericity of aerosol particles and their contribution to radiative forcing. *JQSRT*, 57, 651–68, 1997.
 53. Yu, Y., Notaro, M., Liu, Z., Kalashnikova, O., Alkolibi, F., Fadda, E., and Bakhrjy, F. Assessing temporal and spatial variations in atmospheric dust over Saudi Arabia through satellite, radiometric, and station data, *J. Geophys. Res. Atmos.*, 118, 13, 253–13, 264, 2013.
 54. Yu, Y., Notaro, M., Liu, Z., Wang, F., Alkolibi, F., Fadda, E. and Bakhrjy, F. Climatic controls on the interannual to decadal variability in Saudi Arabian dust activity: Toward the development of a seasonal dust prediction model. *J. Geophys. Res. Atmos.*, 120, 1739–1758, 2015.

834 55. Zhao, G. and Girolamo, L. A cloud fraction versus view angle technique for
835 automatic in-scene evaluation of the MISR cloud mask. J. Appl. Meteorol., 43, 6,
836 860–869, 2004.

837

838

839

840

841 **Tables' caption**

842 Table 1. Geographic location of the AERONET sites used in this study

843 Table 2. Statistics for the calculation of MODIS/Terra, MODIS/Aqua, and MISR with that
844 of AERONET measurements over seven sites in the Middle East and North Africa,
845 including R: correlation coefficient, Gfraction: good fraction; N: number of
846 observations

847 Table 3. Statistics for biomass and mixed sites, parameters as in Table 3. Caption.

848 Table 4. Percentage of AODs retrievals greater than 0.4 recorded by AERONET all data,
849 MISR all data and MODIS matched data over seven AERONET sites in Middle East and
850 North Africa.

851

852

853

854

855

856

857

858

859

860

Deleted: ¶
¶
¶

Deleted: dust sites,

Deleted: RMSE: Root Mean Square deviation;

Deleted: -

Deleted: Table 4. MISR coverage for six days of major dust activity over the Arabian Peninsula during March 2009. ¶

Deleted: 5

Deleted: 8

872

873

874

875

876

877 **Figures caption**

878 Figure 1. Location of the AERONET stations over North Africa and the Middle East. The

879 numbers on the map indicate the site location as 1: Saada, 2: Tamanrasset_INM, 3: Cairo,

880 4: Sede Boker, 5: Solar Village, 6: Mezaira, 7: Bahrain.

881 Figure 2. Scatter plot of MISR AOD versus AERONET AOD based on seasons and

882 aerosols categorization.

883 Figure 3. Scatter plot of MODIS AOD versus AERONET AOD based on seasons and

884 aerosols categorization.

885 Figure 4. Time series of monthly mean AOD derived from MODIS/Aqua, MODIS/Terra,

886 MISR and AERONET over a) dust b) biomass and c) mixed dominated aerosol regions.

887 Figure 5. Long range AOD difference for MODIS/Terra and MODIS/Aqua over the dust,

888 biomass and mixed sites.

889 Figure 6. Histogram of the MISR, MODIS and Solar Village AERONET measurements a)

890 MISR b) MODIS data retrievals.

891 Figure 7. Histogram of the MISR, MODIS and Mezaria AERONET measurements a)

892 MISR b) MODIS data retrievals.

893 Figure 8. Histogram of the MISR, MODIS and Bahrain AERONET measurements a) MISR

894 b) MODIS data retrievals.

895 Figure 9. Histogram of the MISR, MODIS and SAADA AERONET measurements a)

896 MISR b) MODIS data retrievals.

Deleted: s

898 Figure 10. Histogram of the MISR, MODIS and Taman AERONET measurements a)

899 MISR b) MODIS data retrievals.

900 Figure 11. Histogram of the MISR, MODIS and SEDEE Boker AERONET measurements

901 a) MISR b) MODIS data retrievals.

902 Figure 12. Histogram of the MISR, MODIS and Cairo AERONET measurements a) MISR

903 b) MODIS data retrievals.

904

905

906

907

908

909

910

911

912

913

914

915

916

917

918

919

920

921

922

923

924

925

926

927

Table 1.

Location name	Lon./Lat.	Measurement period
Solar Village	24.907° N/46.397° E	2000-2015
Mezaria	23.105° N/53.755° E	2004-2015
Bahrain	26.208° N/50.609° E	2000-2006
Saada	31.626° N/8.156° W	2003-2015
Taman	22.790° N/5.530° E	2000-2015
Cairo	30.081° N/31.290° E	2005 -2007
Sede Boker	30.855° N/34.782 °E	2000-2015

928

929

930

931

932

933

Table 2.

AERONET	Sensor	Season	Mean Value	N	R	Gfraction (%)	
Site							
			AERONET			Satellite	
		DJF	0.31±0.22	0.38±0.20	338	0.94	60.05
		MAM	0.39±0.27	0.45±0.23	89	0.94	65.16
	MISR	JJA	0.39±0.18	0.45±0.17	141	0.90	70.21
		SON	0.27±0.16	0.35±0.14	3	0.99	33.33
Solar Village		DJF	0.27±0.19	0.33±0.17	1500	0.48	51.80

		MAM	0.36±0.24	0.26±0.17	389	0.68	90.23
	MODIS	JJA	0.34±0.17	0.42±0.19	429	0.41	54.31
	Terra	SON	0.22±0.10	0.36±0.12	471	0.51	28.87
		DJF	0.33±0.15	0.40±0.17	60	0.89	75.00
		MAM	0.32±0.19	0.41±0.22	13	0.90	69.23
	MISR	JJA	0.42±0.13	0.47±0.17	21	0.85	80.95
		SON	0.29±0.07	0.36±0.07	22	0.87	77.27
Mezaria		DJF	0.32±0.15	0.35±0.19	198	0.86	74.74
		MAM	0.44±0.33	0.45±0.27	115	0.92	78.07
	MODIS	JJA	0.39±0.14	0.43±0.20	89	0.81	71.91
	Terra	SON	0.28±0.13	0.30±0.16	97	0.87	77.31
		DJF	0.37±0.11	0.31±0.10	17	0.73	100
		MAM	0.31±0.11	0.28±0.14	3	0.89	100
	MISR	JJA	0.40±0.09	0.36±0.09	8	0.69	100
		SON	0.40±0.09	0.30±0.05	4	0.98	100
Bahrain		DJF	0.42±0.29	0.20±0.19	121	0.41	93.38
		MAM	0.50±0.28	0.13±0.15	25	0.26	96.00
	MODIS	JJA	0.55±0.26	0.31±0.27	42	0.50	88.09
	Terra	SON	0.35±0.14	0.21±0.12	29	0.32	93.10

934

935

936

937

Table 3.

AERONET	Sensor	Season	Mean Value		N	R	Gfraction
Site							(%)
			AERONET	Satellite			
		DJF	0.24±0.16	0.22±0.15	149	0.93	97.29
		MAM	0.21±0.13	0.19±0.11	53	0.89	96.15
	MISR	JJA	0.29±0.14	0.27±0.15	80	0.93	97.46
		SON	0.19±0.15	0.19±0.12	60	0.94	98.30

SAADA	DJF	0.23±0.16	0.32±0.21	550	0.57	57.81	
	MAM	0.24±0.18	0.39±0.23	90	0.43	44.44	
	MODIS	JJA	0.30±0.17	0.45±0.18	201	0.40	45.27
	Terra	SON	0.19±0.13	0.22±0.14	162	0.71	72.39
Taman	DJF	0.19±0.23	0.24±0.19	135	0.92	70.89	
	MAM	0.29±0.22	0.35±0.24	24	0.97	82.60	
	MISR	JJA	0.35±0.30	0.39±0.19	36	0.85	71.42
	SON	0.19±0.15	0.19±0.12	60	0.94	98.30	
	DJF	0.19±0.22	0.18±0.16	319	0.67	81.81	
	MODIS	MAM	0.24±0.19	0.22±0.17	67	0.55	83.58
	Terra	JJA	0.37±0.32	0.29±0.20	69	0.69	84.05
	SON	0.14±0.14	0.13±0.10	117	0.54	84.61	
Cairo	DJF	0.33±0.20	0.28±0.11	13	0.94	100	
	MAM	0.22±0.06	0.24±0.08	5	0.99	100	
	MISR	JJA	0.43±0.23	0.34±0.11	5	0.99	100
	SON	0.38±0.21	0.29±0.12	4	0.97	100	
	DJF	0.33±0.16	0.20±0.11	158	0.30	95.56	
	MAM	0.32±0.16	0.12±0.08	39	0.25	100	
	MODIS	JJA	0.35±0.14	0.28±0.07	58	0.17	94.82
	Terra	SON	0.38±0.19	0.20±0.09	29	0.07	93.82
SEDEE_BOKER	DJF	0.14±0.06	0.21±0.07	23	0.87	40.90	
	MAM	0.14±0.05	0.24±0.09	13	0.68	33.33	
	MISR	JJA	0.16±0.05	0.24±0.06	163	0.85	33.33
	SON	0.15±0.07	0.23±0.06	72	0.89	33.80	
	DJF	0.16±0.12	0.23±0.14	1312	0.36	53.50	
	MAM	0.21±0.18	0.24±0.19	338	0.34	65.68	
	MODIS	JJA	0.16±0.09	0.33±0.13	392	0.27	17.34
	Terra	SON	0.16±0.09	0.23±0.12	477	0.46	58.49

940
941
942
943
944
945
946

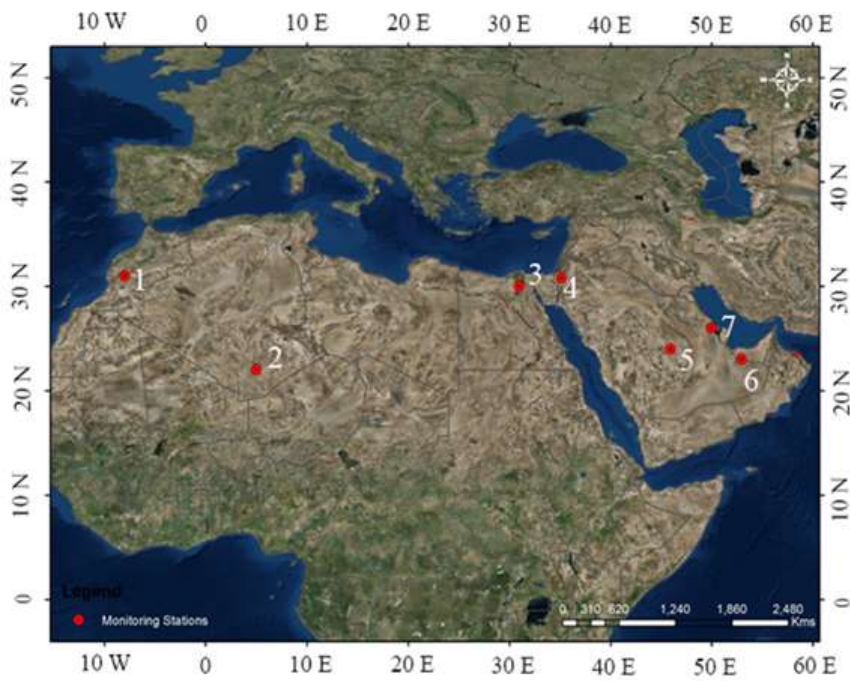
Table 4.

	AERONET		MISR		MODIS	
	AOD		AOD		AOD	
	N	% > 0.4	N	% > 0.4	N	% > 0.4
Solar	3978	28.7	684	32.8	2789	30.1
Village						
Mezaria	1650	30.2	547	45.7	498	40.7
Bahrain	1117	33.3	676	35.7	217	18.4
SAADA	3184	10.8	667	11.5	1004	34.6
Taman	1863	17.9	845	22.6	572	9.4
Cairo	269	53.5	620	17.7	284	4.2
SEDEE	5722	4.8	675	9	2519	12.8

947
948
949
950
951
952
953
954
955

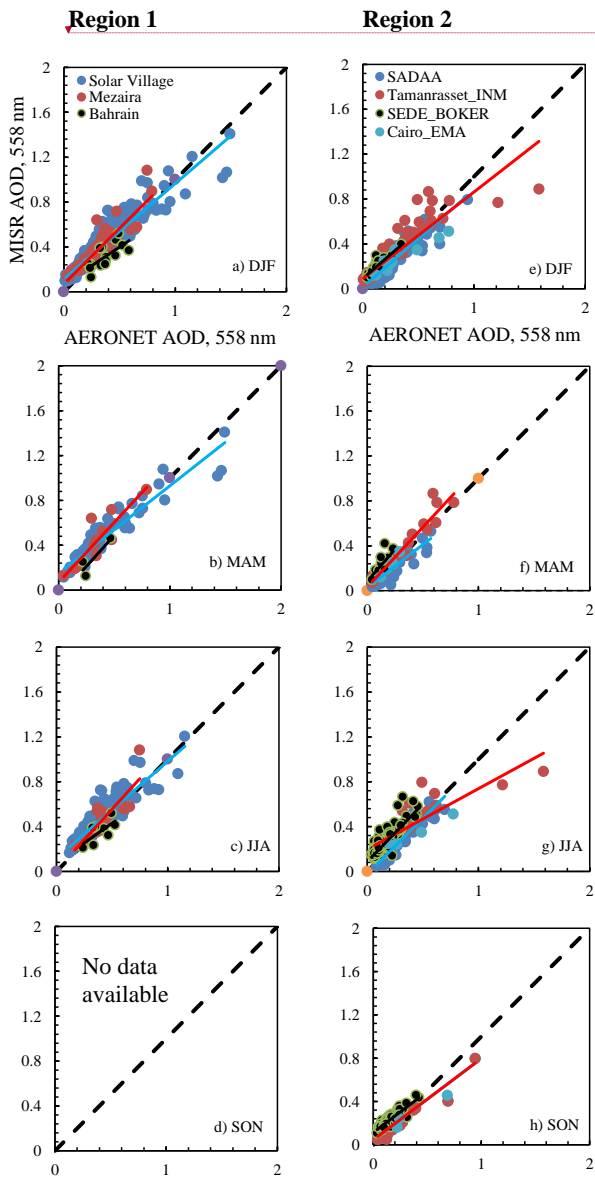
Deleted: ¶

968
969
970
971
972
973
974
975
976
977



978 Figure 1.
979
980
981
982
983

984
985
986
987
988
989
990
991
992
993
994
995
996
997
998
999
1000
1001
1002
1003
1004
1005
1006
1007
1008



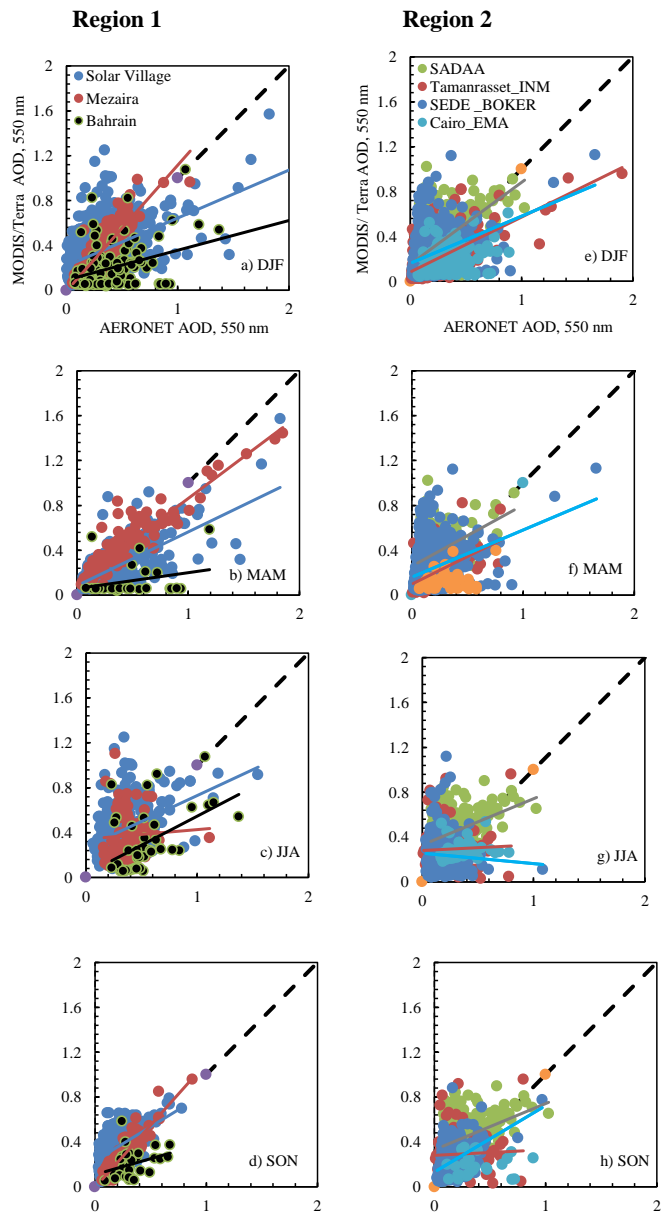
Deleted: ¶
¶
¶

1013

1014

Figure 2.

1015



1021

1022

1023

1024

1025

1026

1027

1028

1029

1030

1031

1032

1033

1034

1035

1036

1037

Figure 3.

1038

1039

1040

1041

1042

1043

1044

1045

1046

1047

1048

1049

1050

1051

1052

1053

1054

1055

1056

1057

1058

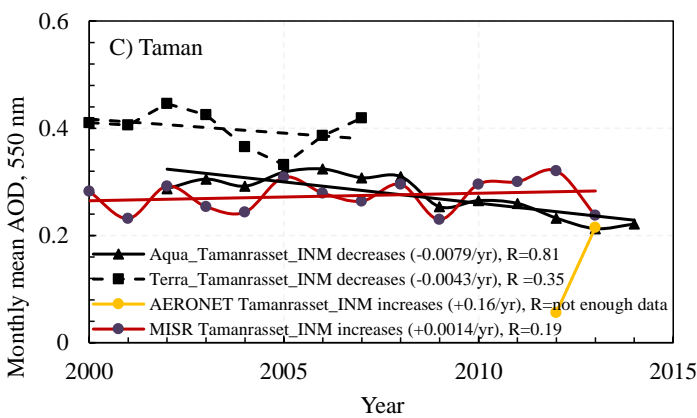
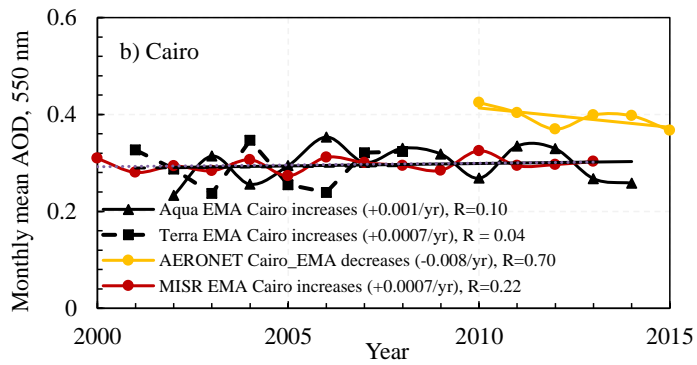
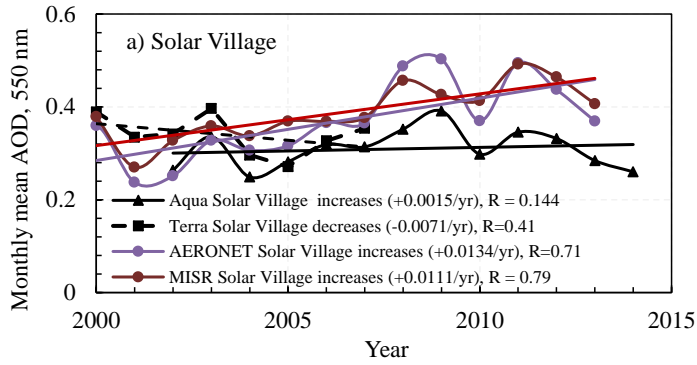
1059

1060

1061

1062

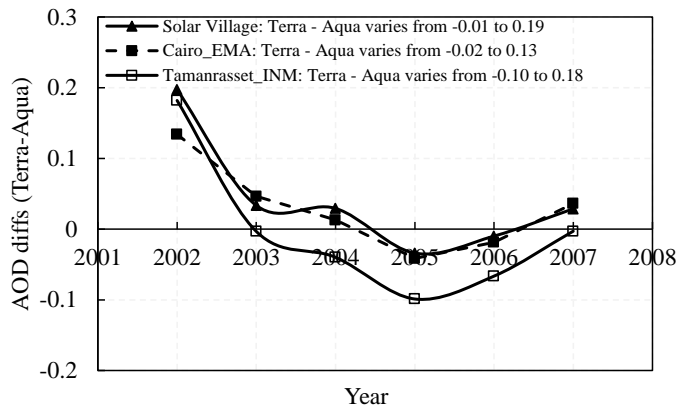
Deleted: ¶



1064

1065 Figure 4.

1066



1075

1076 Figure 5.

1077

1078

1079

1080

1081

1082

1083

1084

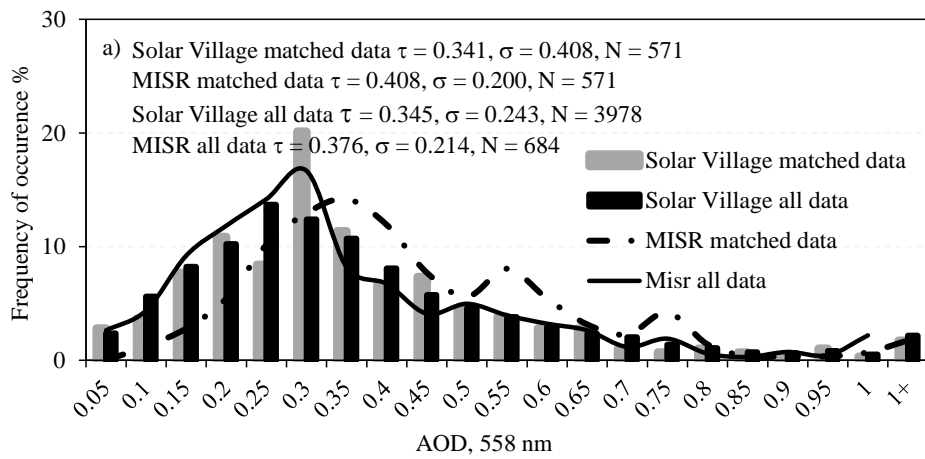
1085

1086

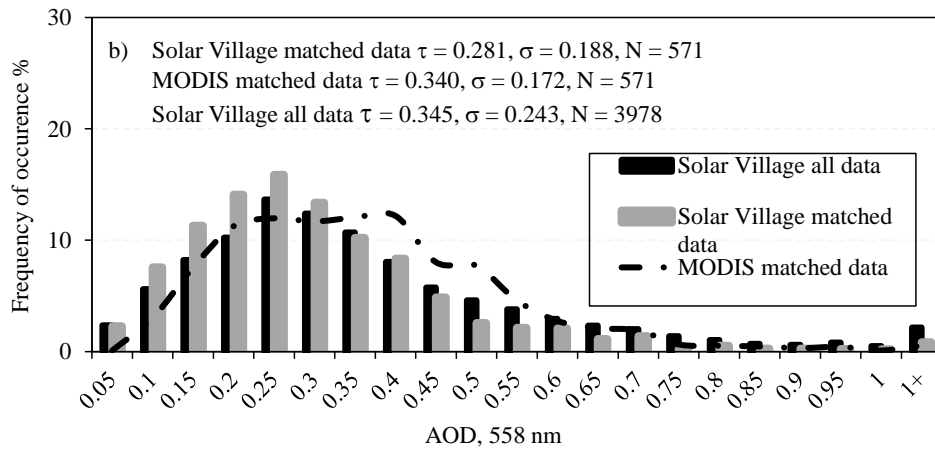
1087

1088

1089
1090
1091



1092

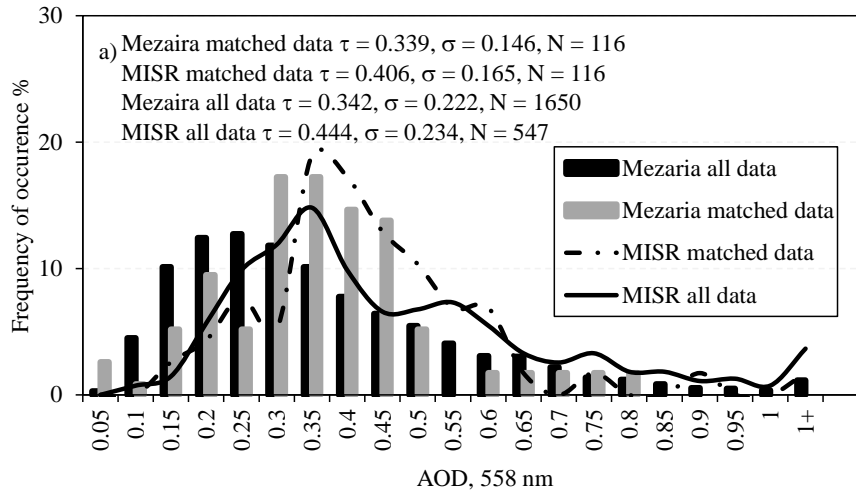


1093

1094 Figure 6.

1095

1096



1097

1098

1099

1100

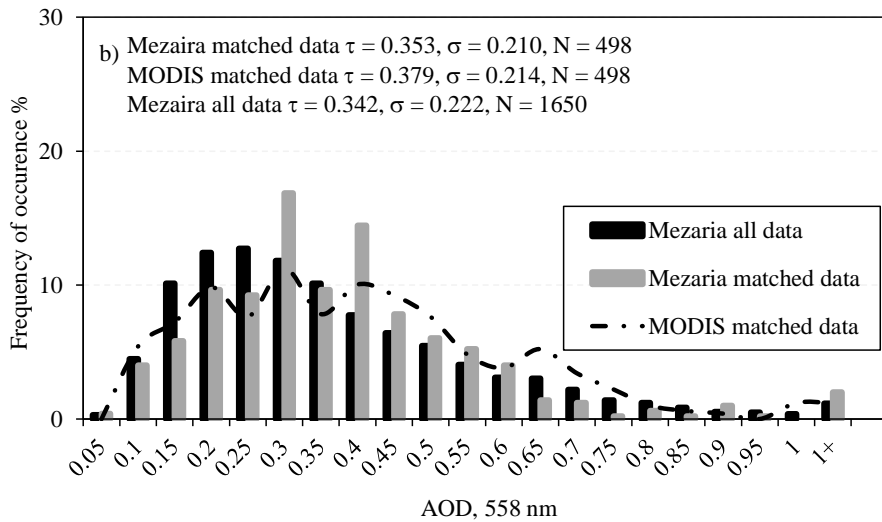
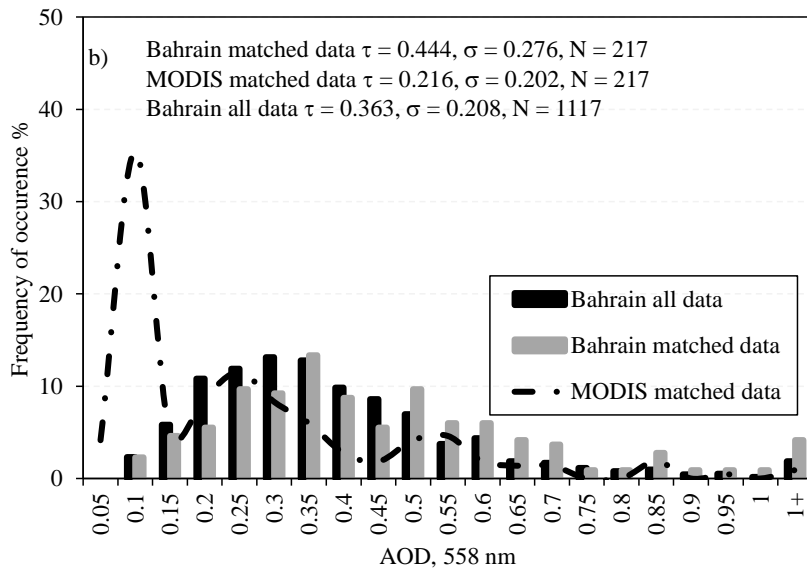
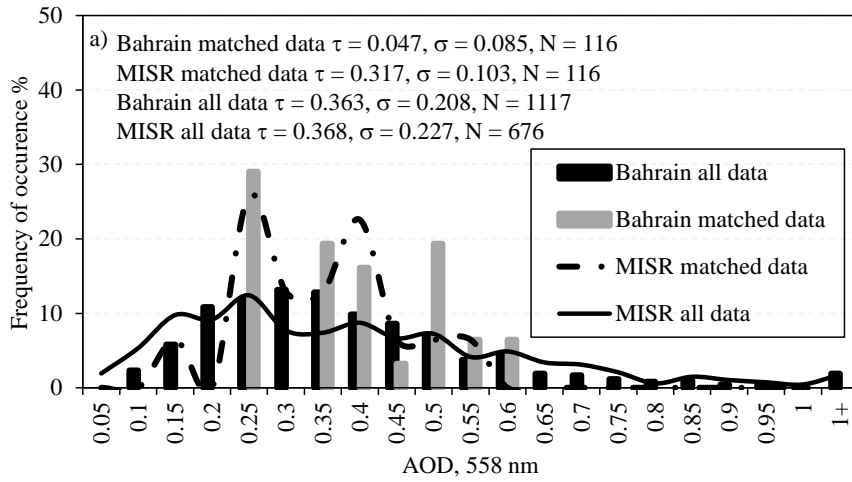


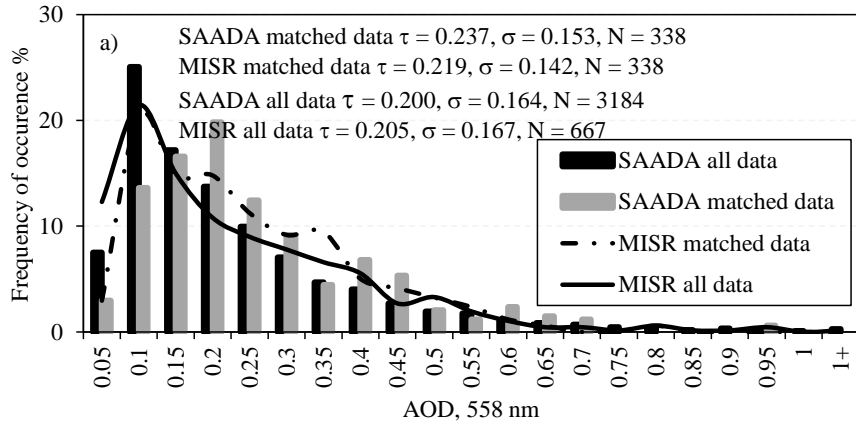
Figure 7.



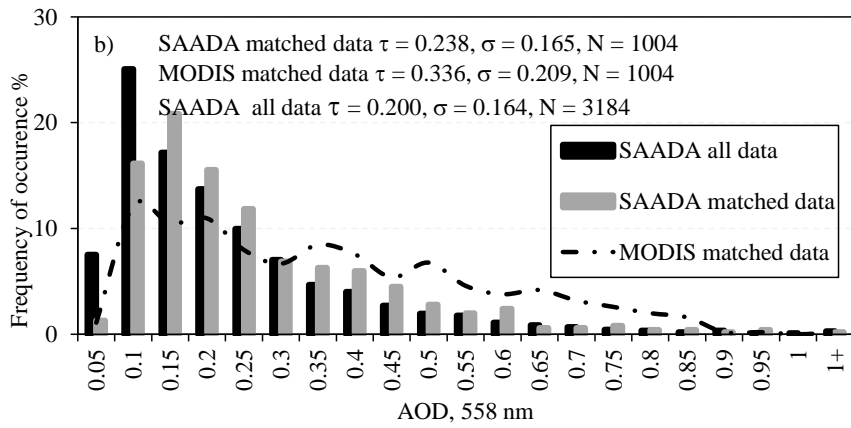
1102 Figure 8.

Deleted: ¶
¶

1106



1107



1108

1109

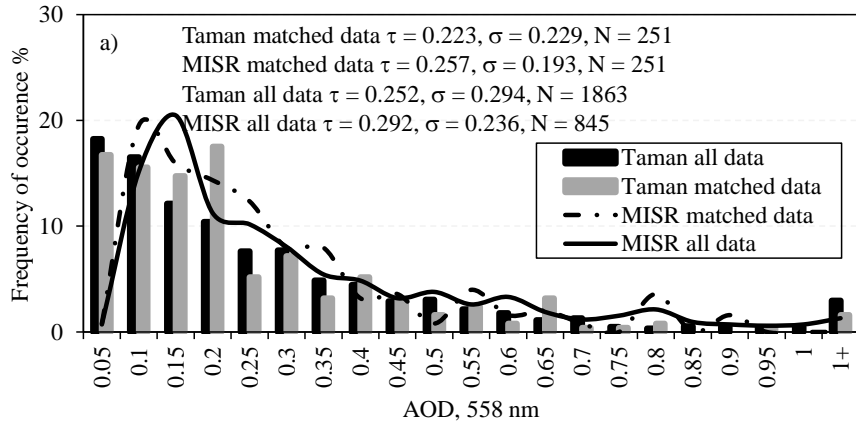
1110 Figure 9.

1111

1112

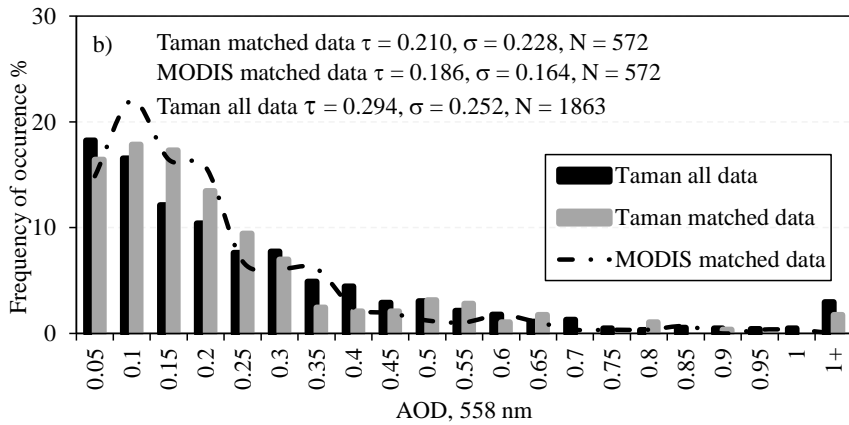
1113

1114



1115

1116



1117

1118

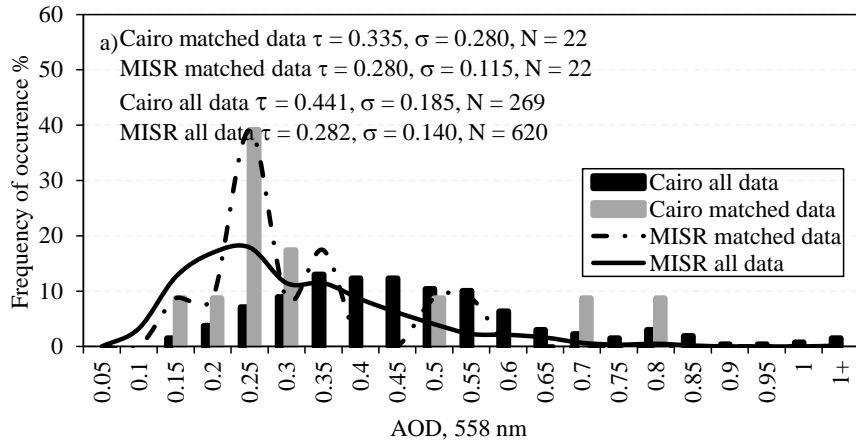
1119

1120 Figure 10.

1121

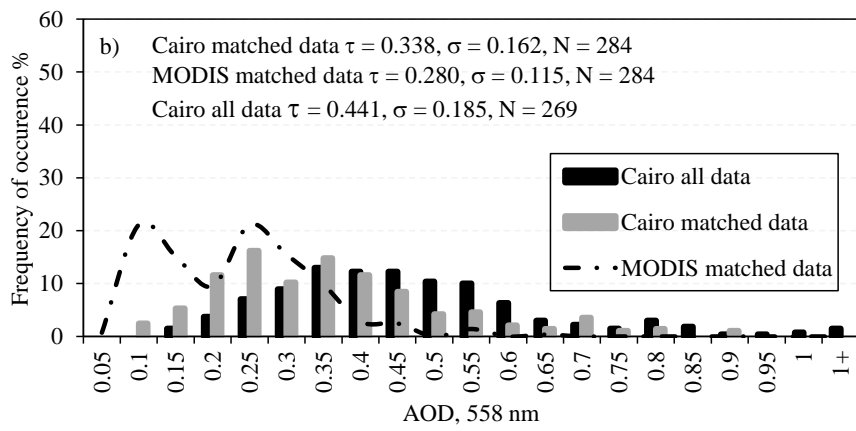
1122

1123



1124

1125



1126

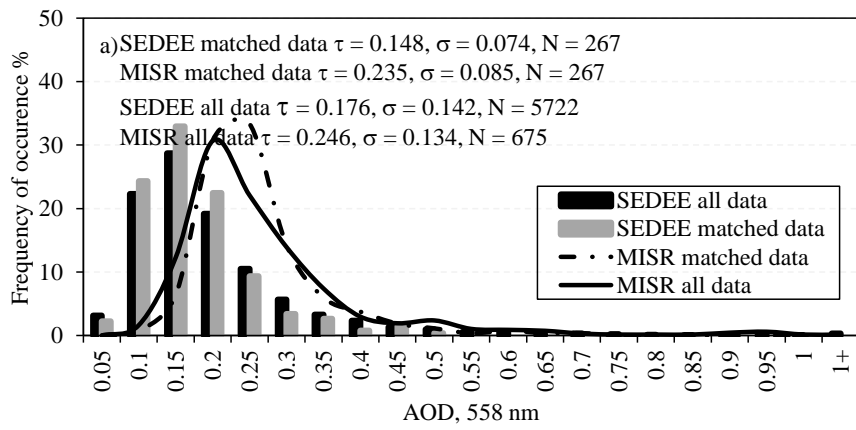
1127

1128

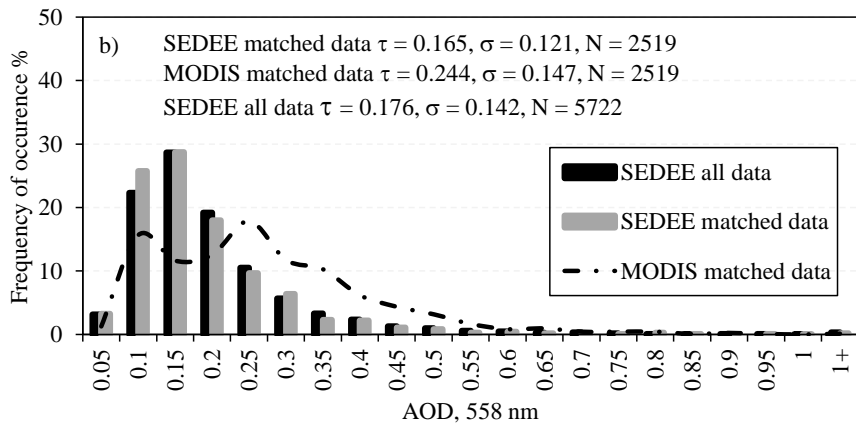
1129

1130 Figure 11.

1131
1132
1133



1134
1135



1136
1137
1138

Figure 12.